# Dalton Transactions

## Accepted Manuscript

This article can be cited before page numbers have been issued, to do this please use: W. liang, C. J. Coghlan, F. Ragon, M. Rubio-Martinez, D. M. D'Alessandro and R. Babarao, *Dalton Trans.*, 2016, DOI: 10.1039/C6DT00189K.


This is an *Accepted Manuscript*, which has been through the Royal Society of Chemistry peer review process and has been accepted for publication.

*Accepted Manuscripts* are published online shortly after acceptance, before technical editing, formatting and proof reading. Using this free service, authors can make their results available to the community, in citable form, before we publish the edited article. We will replace this *Accepted Manuscript* with the edited and formatted *Advance Article* as soon as it is available.

You can find more information about *Accepted Manuscripts* in the Information for Authors.

Please note that technical editing may introduce minor changes to the text and/or graphics, which may alter content. The journal's standard Terms & Conditions and the Ethical guidelines still apply. In no event shall the Royal Society of Chemistry be held responsible for any errors or omissions in this *Accepted Manuscript* or any consequences arising from the use of any information it contains.

ROYAL SOCIETY OF CHEMISTRY

www.rsc.org/dalton

ROYAL SOCIETY OF CHEMISTRY View Article Online
DOI: 10.1039/C6DT00189K

Journal Name

COMMUNICATION



# Defect engineering of UiO-66 for $CO_2$ and $H_2O$ uptake - a combined experimental and simulation study

Received 00th January 20xx,
Accepted 00th January 20xx

DOI: 10.1039/x0xx00000x

www.rsc.org/

Weibin Liang,[a] Campbell J. Coghlan,[b] Florence Ragon,[a] Marta Rubio-Martinez,[c] Deanna M. D'Alessandro[a*] and Ravichandar Babarao[c*]

**Defect concentrations and their compensating groups have been systematically tuned within UiO-66 frameworks by using modified microwave-assisted solvothermal methods. Both of these factors have a pronounced effect on $CO_2$ and $H_2O$ adsorption at low and high pressure.**

Recent studies have shown that, like other solid-state materials, defects can be systematically introduced into the crystal lattice of some canonical metal-organic frameworks (MOFs).[1-5] Such defects may be intrinsic such as crystal imperfections,[6] or may be introduced via ligand replacement with a non-bridging ligand such as hydroxide and solvent molecules.[7, 8] Defects can also be generated *via* surfactant additives or created by substitution of the bridging ligand with secondary ligands,[4, 9, 10] and may be present within a structure as a partially occupied interpenetrated net.[11] Structural disorder and heterogeneity within MOFs breaks the periodic arrangement of atoms and greatly influences the pore/aperture sizes as well as the surface properties of the resulting materials,[12] which subsequently modifies their performance in guest storage/separation, catalysis and proton conductivity.[1, 5, 9, 11-13]

Owing to their attractive thermal, mechanical and chemical stabilities, zirconium (Zr) based UiO MOFs (UiO = University of Olso) with the nominal chemical formula $[Zr_6O_4(OH)_4(L)_6]$ (L = linear dicarboxylate) have gained significant attention and have demonstrated promise for industrial applications.[14, 15] UiO-66, $[Zr_6O_4(OH)_4(bdc)_6]$ (bdc = 1,4-benzenedicarboxylate), comprising six-centred Zr-oxyhydroxide clusters linked *via* linear bdc ligands to form a face-centred cubic (*fcu*) net, is considered as the pristine model for a family of isoreticular structures: Hf, Ce or U can substitute Zr,[2, 16-18] and a number of different dicarboxylates can be used in lieu of the bdc anion.[15, 19]

The first indication of site defects on the $[Zr_6O_4(OH)_4]^{12+}$ SBU was derived from thermogravimetric analysis (TGA) measurements,[3, 20] which suggested that approximately one in 12 of the bdc linkers were missing.[20] This postulation was recently supported through various analyses such as TGA,[2, 3, 12] guest adsorption,[4, 13] nuclear magnetic resonance (NMR),[10] IR/Raman spectroscopy,[3] and X-ray or neutron diffraction.[2, 13]

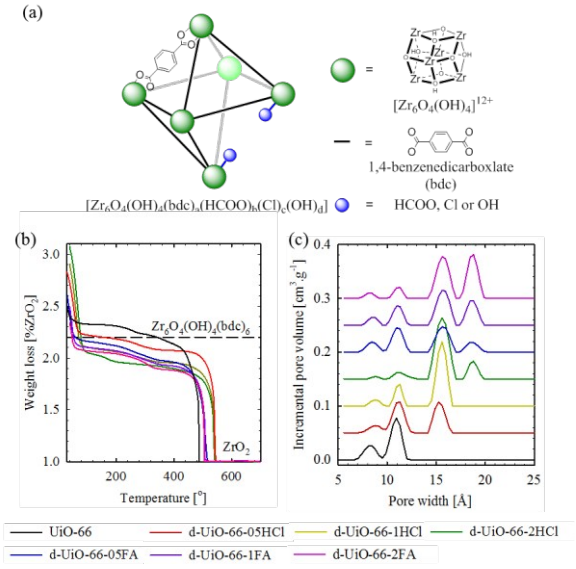


**Figure 1** a) Structural illustration and proposed chemical formula for defective d-UiO-66-aC. Colour scheme: Zr-oxo secondary building unit (SBU, $[Zr_6O_4(OH)_4]^{12+}$) in green; 1,4-benzenedicarboxylate (bdc) in black; formate ($HCOO^-$), chloride ($Cl^-$), and/or hydroxyl ($OH^-$) in blue. b) Normalised thermogravimetric analysis (TGA) for UiO-66 and d-UiO-66-aC samples. Black dashed-line indicates the theoretical weight for perfect UiO-66 at 350 °C. c) Pore-size distribution curves for UiO-66 and d-UiO-66-aC extracted from the $N_2$ adsorption isotherms at 77 K by NLDFT model.

Almost all modified synthesis procedures for UiO-66 in the literature result in missing linker defects.[3] In the present study, formic acid and concentrated hydrochloric acid (conc. HCl) were selected as representative additives for d-UiO-66

[a] School of Chemistry, The University of Sydney, New South Wales 2006, Australia.
[b] Centre for Advanced Nanomaterials, School of Chemistry & Physics, The University of Adelaide, South Australia, Australia.
[c] CSIRO Manufacturing, Private Bag 10, Clayton South MIDS, Victoria 3169, Australia.

Electronic Supplementary Information (ESI) available: [A detailed account of the synthesis procedures, characterisation results, and simulation experiments for perfect and defective is provided in the ESI]. See DOI: 10.1039/c000000x/

synthesis, which differ in their mechanism of defect-generation. Formic acid acts primarily as a monodentate modulator to compete with bidentate bdc ligands for coordination sites on Zr-oxo clusters.[21] In this case, the formation rate of the MOF is decelerated and missing-linker defects are mainly generated *via* incomplete exchange of the pre-loaded formate on the SBUs. By contrast, conc. HCl functions by accelerating the MOF synthesis kinetics, thus favouring the formation of inherent defects either from misconnections or dislocations during crystallisation or from post-crystallisation cleavage.[22, 23] In both cases, missing-linker defects occur in UiO-66 with the concomitant incorporation of formate, chloride and/or hydroxyl anions to the Zr-oxo clusters for charge-compensation.[24] Due to the difference in chemical and physical properties, we suspect that these compensating counter anions are of paramount importance in manipulating the crystal quality, of which literature reports are limited prior to the present work.

Herein, a microwave-assisted solvothermal synthesis protocol was adopted to prepare pure phases of high-quality crystalline d-UiO-66-aC frameworks with different defect concentrations and compensating-ligand compositions (a and C represent the volume (in mL; 05, 1 or 2) and type (HCl = conc. HCl or FA = formic acid) of additives used in synthesis protocols, respectively, see ESI for details).[25, 26] Perfect UiO-66 was synthesised according to the literature procedure.[27, 28] Carbon dioxide adsorption properties of the materials were subsequently investigated to extract correlations between the defect concentration and/or composition. The experimental findings were further corroborated by computational studies. Following MOF synthesis, the frameworks were washed with *N,N'*-dimethylformamide (DMF, 3 × 20 mL), methanol (3 × 20 mL), and acetone (3 × 20 mL) and dried *in vacuo*. Notably, in the microwave protocol, the introduction of $H_2O$ is crucial for obtaining a pure UiO-66 phase, without which a polymorphous MIL-140A phase appears even at low synthesis temperatures (140 °C).

The defective UiO-66 samples were first characterised by X-ray powder diffraction (XRPD) to study their crystallinity and stability (ESI). All six d-UiO-66 samples (d-UiO-66-05HCl, d-UiO-66-1HCl, d-UiO-66-2HCl, d-UiO-66-05FA, d-UiO-66-1FA, and d-UiO-66-2FA) shared an identical XRPD pattern to that of UiO-66 which was qualitatively indicated by *Le Bail* fittings (ESI).

The concentration of missing linker defects and the composition of their compensating-ligands were further systematically studied *via* TGA, energy dispersive spectroscopy (EDS), and $^1$H NMR (see ESI for details). The chemical formulae for UiO-66 and d-UiO-66-aC are listed in Table S4 (ESI). Notably, the overall chemical compositions for d-UiO-66-aCs calculated in this work may not precisely reflect the atomic composition of the defect sites, which have been studied *via* simulation or single-crystal diffraction in literature.[24,29]

As expected for d-UiO-66-aCs, a higher dosage of conc. HCl or formic acid results in a higher defect concentration, as evidenced by TGA analysis (Figure 1b) and the molecular formula calculations (the number of bdc ligands drop from 6 (theoretical value) to 4.60 and 4.46 in the most defective d-UiO-66-2HCl and d-UiO-66-2FA samples, respectively, Table S4 (ESI)). A further increase in the conc. HCl dosage from 2 mL (d-UiO-66-4HCl and d-UiO-66-6HCl, ESI) did not result in more-defective samples, indicating the maximum missing-linker amount (around 3 out of 12 bdcs are missing in each Zr-oxo cluster).[30, 31] The surface area and pore volume of perfect UiO-66 are qualitatively consistent with the reported theoretical values (Table 1),[32] however, for d-UiO-66-aCs, they systematically increase as a function of the defect-concentration (Table 1). d-UiO-66-2FA represents the highest BET surface area (1789 $m^2.g^{-1}$) value for the UiO-66(Zr) samples.[33]

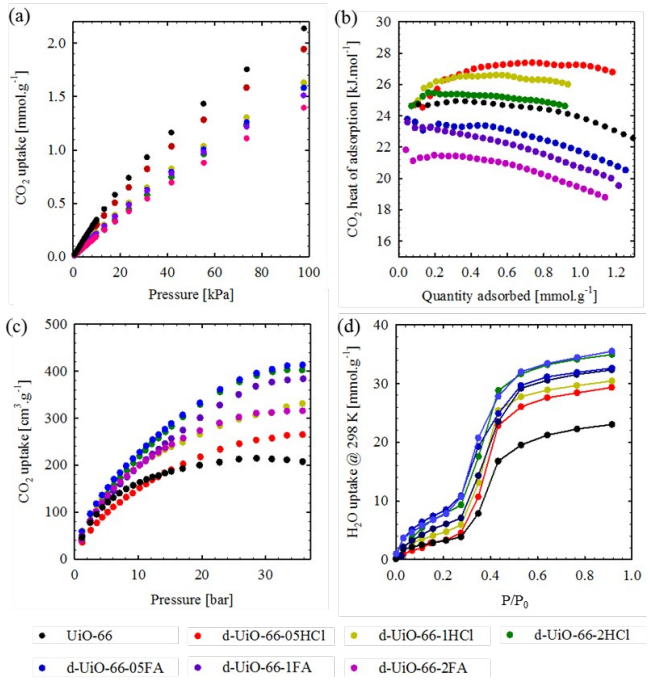


**Figure 2** (a) $CO_2$ adsorption isotherms (up to 1 bar) at 298 K; (b) Isosteric heat of $CO_2$ adsorption ($|Q_{st}|$ for d-UiO-66-aC frameworks; (c) CO2 adsorption isotherms at 298 K (up to 35 bar) for d-UiO-66-aC; (d) Water adsorption isotherms measured at 298 K for d-UiO-66-aC.

Pore size distributions for d-UiO-66-aCs, obtained by non-local density functional theory (NLDFT, based on *N2 – Cylindrical Pores – Oxide Surface model*) show four main pore sizes centred at *ca.* 8.2, 11.0, 16.0, and 19.0 Å, which are interpreted as tetrahedral and octahedral cages in the pristine UiO-66 structure as well as two different defect-related nano-regions, respectively.[2, 14, 22] As a function of the additive dosage, the proportion of the tetrahedral and octahedral cages in d-UiO-66-aCs decrease, while the nano-cages increase systematically. Interestingly, the secondary nano-regions (~2 nm) in d-UiO-66-aFAs only appeared in d-UiO-66-2HCl with the highest conc. HCl dosage. The pore size distribution results for the d-UiO-66-aCs are qualitatively consistent with computational calculations in the literature.[34] In addition, the presence of nano-regions in the defective UiO-66 samples (Figure 1c) indicates the existence of *reo* type defects (with ~ 17 Å cavities) in these materials.[34]

At 1 bar and 298 K, the maximum $CO_2$ uptake for UiO-66 and d-UiO-66-aCs decreased in the order UiO-66 > d-UiO-66-05HCl > d-UiO-66-1HCl > d-UiO-66-2HCl and d-UiO-66-05FA > d-UiO-66-1FA > d-UiO-66-2FA (Figure 2a and Table 1). For $CO_2$ adsorption at low pressure (< 5 bar), the uptake capacity is mainly related to the $CO_2$-sorbent interactions.[35-38] Perfect UiO-66 with the least structural defects (ESI) and lowest pore volume/specific surface area (Table 1) represents the highest $CO_2$ capacity at 1 bar (2.16 mmol.g$^{-1}$). The effect of the defect concentration and compensating-groups on $CO_2$ adsorption is more obvious in the $CO_2$ isosteric heats of adsorption ($Q_{st}$), which were calculated using the Clausius-Clapeyron equation (Figure 2b). At 1 mmol.g$^{-1}$ $CO_2$ loading, the $Q_{st}$ decreased in the order d-UiO-66-05HCl > d-UiO-66-1HCl > d-UiO-66-2HCl > d-UiO-66-05FA $\approx$ d-UiO-66-1FA > d-UiO-66-2FA. The decreases in $Q_{st}$ observed for d-UiO-66-aCs (as a function of increasing additive dosage) are attributed to their enlarged cavity sizes (Figure 1c) originating from missing-linker defects. With a similar amount of defects (Figure 1b and ESI), $Q_{st}$ for d-UiO-66-2HCl is ~5 kJ. mol$^{-1}$ higher than that for d-UiO-66-1FA, which cannot be explained solely by the similar pore size distributions, BET surface areas and/or pore volumes (Figure 1c and Table 1). In addition, compared with perfect UiO-66, conc. HCl modified d-UiO-66-aHCls are characterised by higher $Q_{st}$ values relative to the formic acid modified samples. The origin of this difference is primarily ascribed to different interactions between the $CO_2$ molecules and the $OH^-$, $Cl^-$ and/or $HCOO^-$ which charge-compensate the defective Zr-oxo cluster. DFT calculations indicate that the binding energy for $CO_2$ to perfect and defective Zr-clusters decreases in the order -OH (-36 kJ.mol$^{-1}$) > -Cl (-31.06 kJ.mol$^{-1}$) > perfect (-30.32 kJ.mol$^{-1}$) > -OOCH (-29.55 kJ.mol$^{-1}$), which is qualitatively consistent with the trend in our experimental $Q_{st}$ results (see section S5 in ESI for detail).

**Table 1** Comparison of physical properties and $CO_2$ adsorption performance of d-UiO-66-aCs.

| Entry[a] | $S_{BET}$[b] | $V_{total}$[c] | $n_{CO2, 1bar}$[d] | $n_{CO2, 35bar}$[e] |
|---|---|---|---|---|
| UiO-66$_{sim}$[39] | 1283 | 0.45 | - | - |
| UiO-66 | 1127.2(3) | 0.44 | 2.16 | 207.20 |
| 1-05HCl | 1376.6(9) | 0.54 | 1.97 | 265.07 |
| 1-1HCl | 1427.1(11) | 0.59 | 1.66 | 342.39 |
| 1-2HCl | 1652.1(16) | 0.71 | 1.61 | 405.90 |
| 1-05FA | 1355.7(9) | 0.60 | 1.61 | 413.12 |
| 1-1FA | 1590.8(14) | 0.69 | 1.54 | 383.62 |
| 1-2FA | 1789.3(16) | 0.95 | 1.42 | 336.94 |

[a]1 = d-UiO-66; [b]in m$^2$.g$^{-1}$, calculated from the $N_2$ adsorption isotherms measured at 77 K. Values in parentheses indicate the uncertainties; [c]in cm$^3$.g$^{-1}$, calculated from the amount of $N_2$ at 1 bar at 77 K; [d]in mmol.g$^{-1}$, measured at 298K; [e]in cm$^3$.g$^{-1}$, measured at 298K.

Similar to other MOFs, the high-pressure $CO_2$ adsorption results for UiO-66 and d-UiO-66-aC are proportional to their BET surface areas (Figure 2c and Figure S20). At 35 bar and 298 K, the $CO_2$ gravimetric capacity decreased in the order d-UiO-66-05FA > d-UiO-66-2HCl > d-UiO-66-1FA > d-UiO-66-1HCl > d-UiO-66-2FA > d-UiO-66-05HCl > UiO-66 (Figure 2c and Table 1). For UiO-66 and d-UiO-66-aHCls, this trend is consistent with previously reported results for other MOFs in which the enlargement in the framework pore size enhances the high-pressure $CO_2$ capacity.[40]

For d-UiO-66-aFAs, despite the increase in pore volume as a function of formic acid usage, the $CO_2$ capacity decreases. Among the studied samples, d-UiO-66-05FA represents the highest $CO_2$ adsorption capacity at 35 bar (413.12 cm$^3$.g$^{-1}$ or 44.8 wt%). Considering the moderate BET surface area and pore volume of d-UiO-66-05FA, it is likely that the high $CO_2$ capacity is due to the average pore diameter being of an optimal size to confine $CO_2$ molecules. Despite the variation of defect concentration and compensating groups, d-UiO-66-aCs retain their crystallinity after high-pressure $CO_2$ sorption studies.

As illustrated in Figure 2d, the missing-linker defects can also drastically affect the hydroscopic properties of resulting materials. In general, ideal UiO-66 is more hydrophobic than defective samples.[41, 42] The water isotherm of ideal UiO-66 has a sigmoidal shape with a water condensation pressure at $P/P_0$ = 0.3 at 298 K (Figure 2d). However, for defective UiO-66 samples, the step pressure shifts to lower values as a function of the defect amount, indicating that the missing organic ligands in UiO-66 make the MOFs more hydrophilic (Figure 2d). The graph of derivative water adsorption *vs.* relative humility (ESI) shows that the major water adsorption occurs at $P/P_0$ = 0.3 for UiO-66, d-UiO-66-05HCl, and d-UiO-66-1HCl. However, for d-UiO-66-2HCl and d-UiO-66-aFAs, another adsorption at $P/P_0 \approx 0.27$ appears, which is consistent with the appearance of the second 2 nm defect-related region in these samples. In addition, at $P/P_0$ = 0.9 and 298 K, the maximum water uptake increases in the order of UiO-66 < d-UiO-66-05HCl < d-UiO-66-1HCl < d-UiO-66-05FA < d-UiO-66-1FA < d-UiO-66-2HCl < d-UiO-66-2FA, which coincides with the increase in the defect concentration in the samples. Thus, unlike the missing-linker concentration and pore-size distribution, the type of compensating group does not have a marked effect on the hydroscopic properties of defective UiO-66s.

In conclusion, the synthesis and characterisation of a series of defective UiO-66(Zr) frameworks has demonstrated the relationship between defect concentration/composition and $CO_2$ uptake abilities over both at low and high pressure ranges. In principle, defect-free UiO-66 is ideal for $CO_2$ separation below 1 bar, while defective UiO-66 is superior for high pressure $CO_2$ storage. In addition, conc. HCl modified d-UiO-66-aHCls show higher $CO_2$ affinities than those incorporating formic acid. The presented experimental $CO_2$ sorption studies are qualitatively consistent with the computational results in a recent publication.[34] In addition, water adsorption isotherms illustrate that defects in the form of missing linkers make this MOF more hydrophilic. Computational and experimental

results of $CO_2$ adsorption indicate that not only the amount of defects but also their charge-compensating groups within the materials have a marked effect on the loading of guest molecules. More importantly, the present work illustrates that instead of exploring MOFs with new topologies and/or functionalities, systematically tuning the defect concentration and the compensating groups in frameworks is a powerful tool to obtain novel materials for designed applications.

This research was supported by the Science and Industry Endowment Fund (SIEF). The authors thank A/Profs. Chris Sumby and Christian Doonan at the University of Adelaide, and Prof. Cameron Kepert at the University of Sydney for invaluable instrumental support. The authors also acknowledge the facilities and the scientific and technical assistance of the Australian Microscopy & Microanalysis Research Facility at the Australian Centre for Microscopy & Microanalysis at the University of Sydney. RB acknowledges the computational facilities and services provided through the CSIRO Advanced Scientific Computing, National Computing Infrastructure (NCI) and Pawsey supercomputing facilities.

## Notes and references


1 O. Kozachuk, I. Luz, F. X. Llabres i. Xamena, H. Noei, M. Kauer, H. B. Albada, E. D. Bloch, B. Marler, Y. Wang, M. Muhler and R. A. Fischer, Angew. Chem., Int. Ed., 2014, 53, 7058-7062.

2 M. J. Cliffe, W. Wan, X. Zou, P. A. Chater, A. K. Kleppe, M. G. Tucker, H. Wilhelm, N. P. Funnell, F.-X. Coudert and A. L. Goodwin, Nat. Commun., 2014, 5, 4176.

3 G. C. Shearer, S. Chavan, J. Ethiraj, J. G. Vitillo, S. Svelle, U. Olsbye, C. Lamberti, S. Bordiga and K. P. Lillerud, Chem. Mater., 2014, 26, 4068-4071.

4 J. Park, Z. U. Wang, L.-B. Sun, Y.-P. Chen and H.-C. Zhou, J. Am. Chem. Soc., 2012, 134, 20110-20116.

5 A. Dhakshinamoorthy, M. Alvaro, P. Horcajada, E. Gibson, M. Vishnuvarthan, A. Vimont, J.-M. Greneche, C. Serre, M. Daturi and H. Garcia, ACS Catal., 2012, 2, 2060-2065.

6 L. Carlucci, G. Ciani, M. Moret, D. M. Proserpio and S. Rizzato, Angew. Chem., Int. Ed., 2000, 39, 1506-1510.

7 S. Oeien, D. Wragg, H. Reinsch, S. Svelle, S. Bordiga, C. Lamberti and K. P. Lillerud, Cryst. Growth Des., 2014, 14, 5370-5372.

8 N. Planas, J. E. Mondloch, S. Tussupbayev, J. Borycz, L. Gagliardi, J. T. Hupp, O. K. Farha and C. J. Cramer, J. Phys. Chem. Lett., 2014, 5, 3716-3723.

9 B. Bueken, H. Reinsch, N. Reimer, I. Stassen, F. Vermoortele, R. Ameloot, N. Stock, C. E. A. Kirschhock and D. De Vos, Chem. Commun., 2014, 50, 10055-10058.

10 F. Vermoortele, B. Bueken, G. Le Bars, B. Van de Voorde, M. Vandichel, K. Houthoofd, A. Vimont, M. Daturi, M. Waroquier, V. Van Speybroeck, C. Kirschhock and D. E. De Vos, J. Am. Chem. Soc., 2013, 135, 11465-11468.

11 S. Yang, X. Lin, W. Lewis, M. Suyetin, E. Bichoutskaia, J. E. Parker, C. C. Tang, D. R. Allan, P. J. Rizkallah, P. Hubberstey, N. R. Champness, K. M. Thomas, A. J. Blake and M. Schroder, Nat. Mater., 2012, 11, 710-716.

12 J. M. Taylor, S. Dekura, R. Ikeda and H. Kitagawa, Chem. Mater., 2015, 27, 2286-2289.

13 H. Wu, Y. S. Chua, V. Krungleviciute, M. Tyagi, P. Chen, T. Yildirim and W. Zhou, J. Am. Chem. Soc., 2013, 135, 10525-10532.

14 J. H. Cavka, S. Jakobsen, U. Olsbye, N. Guillou, C. Lamberti, S. Bordiga and K. P. Lillerud, J. Am. Chem. Soc., 2008, 130, 13850-13851.

15 M. Kim and S. M. Cohen, CrystEngComm, 2012, 14, 4096-4104.

16 C. Falaise, C. Volkringer, J.-F. Vigier, N. Henry, A. Beaurain and T. Loiseau, Chem. Eur. J., 2013, 19, 5324-5331.

17 K. E. de Krafft, W. S. Boyle, L. M. Burk, O. Z. Zhou and W. Lin, J. Mater. Chem., 2012, 22, 18139-18144.

18 M. Lammert, M. T. Wharmby, S. Smolders, B. Bueken, A. Lieb, K. A. Lomachenko, D. D. Vos and N. Stock, Chem. Commun., 2015, 51, 12578-12581.

19 W. Lu, Z. Wei, Z.-Y. Gu, T.-F. Liu, J. Park, J. Park, J. Tian, M. Zhang, Q. Zhang, T. Gentle Iii, M. Bosch and H.-C. Zhou, Chem. Soc. Rev., 2014, 43, 5561-5593.

20 L. Valenzano, B. Civalleri, S. Chavan, S. Bordiga, M. H. Nilsen, S. Jakobsen, K. P. Lillerud and C. Lamberti, Chem. Mater., 2011, 23, 1700-1718.

21 A. Schaate, P. Roy, A. Godt, J. Lippke, F. Waltz, M. Wiebcke and P. Behrens, Chem. Eur. J., 2011, 17, 6643-6651.

22 M. J. Katz, Z. J. Brown, Y. J. Colon, P. W. Siu, K. A. Scheidt, R. Q. Snurr, J. T. Hupp and O. K. Farha, Chem. Commun., 2013, 49, 9449-9451.

23 F. Ragon, P. Horcajada, H. Chevreau, Y. K. Hwang, U. H. Lee, S. R. Miller, T. Devic, J.-S. Chang and C. Serre, Inorg. Chem., 2014, 53, 2491-2500.

24 M. Vandichel, J. Hajek, F. Vermoortele, M. Waroquier, D. E. De Vos and V. Van Speybroeck, CrystEngComm, 2015, 17, 395-406.

25 W. Liang and D. M. D'Alessandro, Chem. Commun., 2013, 49, 3706-3708.

26 W. Liang, R. Babarao and D. M. D'Alessandro, Inorg. Chem., 2013, 52, 12878-12880.

27 G. C. Shearer, S. Chavan, J. Ethiraj, J. G. Vitillo, S. Svelle, U. Olsbye, C. Lamberti, S. Bordiga and K. P. Lillerud, Chem. Mater., 2014, 26, 4068-4071.

28 P. S. Barcia, D. Guimaraes, P. A. P. Mendes, J. A. C. Silva, V. Guillerm, H. Chevreau, C. Serre and A. E. Rodrigues, Microporous Mesoporous Mater., 2011, 139, 67-73.

29 C. A. Trickett, K. J. Gagnon, S. Lee, F. Gandara, H.-B. Buergi and O. M. Yaghi, Angew. Chem., Int. Ed., 2015, 54, 11162-11167.

30 M. J. Cliffe, J. A. Hill, C. A. Murray, F.-X. Coudert and A. L. Goodwin, Phys. Chem. Chem. Phys., 2015, Ahead of Print.

31 F. Vermoortele, B. Bueken, G. Le Bars, B. Van de Voorde, M. Vandichel, K. Houthoofd, A. Vimont, M. Daturi, M. Waroquier, V. Van Speybroeck, C. Kirschhock and D. E. De Vos, J. Am. Chem. Soc., 2013, 135, 11465-11468.

32 Q. Yang, V. Guillerm, F. Ragon, A. D. Wiersum, P. L. Llewellyn, C. Zhong, T. Devic, C. Serre and G. Maurin, Chem. Commun., 2012, 48, 9831-9833.

33 Z. Hu, S. Faucher, Y. Zhuo, Y. Sun, S. Wang and D. Zhao, Chem. - Eur. J., 2015, Ahead of Print.

34 A. W. Thornton, R. Babarao, A. Jain, F. Trousselet and F. X. Coudert, Dalton Trans., 2015, Ahead of Print.

35 W. Liang, R. Babarao, T. L. Church and D. M. D'Alessandro, Chem. Commun., 2015, 51, 11286-11289.

36 Y.-S. Bae and R. Q. Snurr, Angew. Chem., Int. Ed., 2011, 50.

37 P. Nugent, Y. Belmabkhout, S. D. Burd, A. J. Cairns, R. Luebke, K. Forrest, T. Pham, S. Ma, B. Space, L. Wojtas, M. Eddaoudi and M. J. Zaworotko, Nature, 2013, 495, 80-84.

38 S. D. Burd, S. Ma, J. A. Perman, B. J. Sikora, R. Q. Snurr, P. K. Thallapally, J. Tian, L. Wojtas and M. J. Zaworotko, J. Am. Chem. Soc., 2012, 134, 3663-3666.

39 P. Ghosh, Y. J. Colon and R. Q. Snurr, Chem. Commun., 2014, 50, 11329-11331.




 

View Article Online
DOI: 10.1039/C6DT00189K

40 Q. Yang, V. Guillerm, F. Ragon, A. D. Wiersum, P. L. Llewellyn, C. Zhong, T. Devic, C. Serre and G. Maurin, Chem. Commun., 2012, 48, 9831-9833.
41 P. Ghosh, Y. J. Colon and R. Q. Snurr, Chem. Commun., 2014, 50, 11329-11331.
42 H. Furukawa, F. Gandara, Y.-B. Zhang, J. Jiang, W. L. Queen, M. R. Hudson and O. M. Yaghi, J. Am. Chem. Soc., 2014, 136, 4369-4381.

View Article Online
DOI: 10.1039/C6DT00189K



## Table of Contents

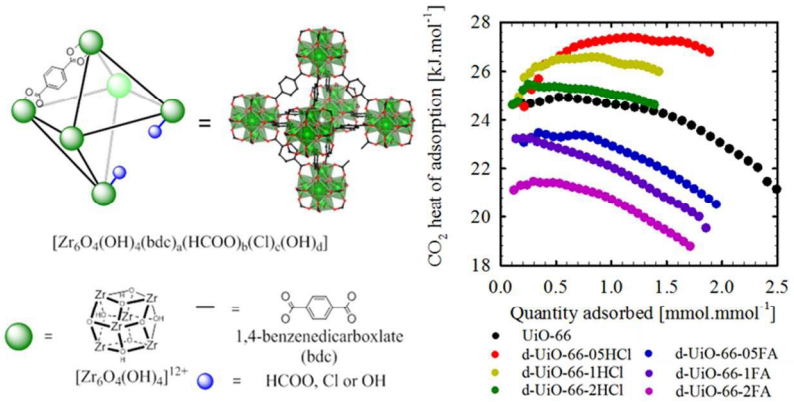


Defect concentrations and their compensating groups have been systematically tuned within UiO-66 frameworks and are found to have a pronounced effect on $CO_2$ and $H_2O$ adsorption at low and high pressure.